Meteorological conditions during SSW events

Project report

Module Upper Atmosphere
summer semester 2020

M.Sc. Meteorologie

submitted by:

Benedikt Gast
Matriculation number: 3739615

16.10.2020

Contents

Chapter 1

Introduction

1.1 Sudden Stratospheric Warmings

Sudden stratospheric warmings (SSWs) are disturbations of the usual stratospheric wintertime circulation which influence the mesospheric circulation as well.
During undisturbed winters the stratopause is situated in altitudes between 55 and 60 km. The stratospheric jet is eastward and the mesospheric jet westward throughout the winter. The zero wind line remains near 75 km (Chandran et al., 2014).
During SSWs, up- and westward propagating planetary (or Rossby) waves from the troposphere amplify and act to weaken the background mean winds. The stratospheric winds flow westward whereby westward propagating gravity waves (GWs) are now being blocked. Due to the GW filtering (see below), only eastward GWs penetrate to the mesosphere, reversing the zonal mean mesospheric flow from westward to eastward - sometimes even the mesospheric jet as well. In some cases after an SSW the stratopause reforms at higher altitudes at around 75 km. This phenomenon is often referred to as elevated stratopause (ES) (Chandran et al., 2014).

1.2 Gravity wave filtering and gravity wave drag

The vertical propagation and dissipation as well as the exerted drag force of GWs plays an important role for the circulation in the mesosphere (McLandress, 1998). The basics of GW filtering are presented in this section.
The dispersion relation

$$m^2 = \frac{N^2}{(c-U)^2} \tag{1.1}$$

relates the vertical wavenumber m to the squares of the buoyancy frequency N and the difference of the zonal phase speed of the GW c and the zonal component of the background wind U (McLandress, 1998).
The background wind determines the vertical propagation of GWs. As it can be seen in equation 1.1, a critical level exists where the zonal phase speed c equals the zonal background wind U. In this case the vertical wavenumber m goes to infinity, which leads to either the absorption or reflection of the GW in this layer. In both cases the wave can't propagate further upward. This process is called "critical layer filtering" of GWs. If c and U have different signs their difference will never become small or 0. As a result GWs with other sign of the phase speed

than the background wind won't be filtered and can propagate further upward. GWs with a phase speed with same sign as the background wind are filtered if c is approximately equal U (McLandress, 1998).
The other way around GWs influence the background wind as well. A steady undamped wave exerts no force on the mean state. But during dissipation the momentum flux of the GW decreases with height. Because of that a mean force on the background wind arises, the gravity wave drag (McLandress, 1998).
As this project adresses SSW events, which occur during wintertime, this consideration is restricted to the winter situation. At first, GWs with various zonal phase speeds - generated near the surface - are considered. Because of the prevailing westerly winds ($U > 0$) in the stratosphere during winter, only eastward travelling waves ($c > 0$) are filtered. Westward travelling GWs ($c < 0$) can propagate up to the mesosphere. As the wave amplitude grows exponentially with height those waves reaching the mesosphere will break there because of their large amplitudes as well. Their dissipation generates a negative force on the zonal background wind. Thus the westerly background wind is decelerated (McLandress, 1998).

1.3 Inter-hemispheric coupling

The effects of an SSW event on the summer hemisphere (in the considered cases this is the southern hemisphere, SH) are related to a process called "inter-hemispheric coupling".
During an SSW event the eastward zonal wind decreases. On the one hand this leads to a Doppler-shifting of the westward propagating GWs (negative phase speeds) towards shorter vertical wavelengths. As a result they break at lower altitudes. On the other hand, GWs with high positive phase speeds can propagate further upward into the mesosphere as they are not filtered any more. Because of these processes the westward GW drag is both reduced and downward shifted in the winter mesosphere (Körnich and Becker, 2010).
Thus the poleward meridional flow on the northern hemisphere (NH) weakens around the SSW onset. As a result the polar mesosphere is cooler and the tropical mesosphere is warmer. Because of the warmer tropical mesosphere the latitudinal gradient in the mesosphere of the summer hemisphere is weakened. In order to fulfill the thermal wind balance the westward zonal wind on the SH has to weaken as well. Therefore GWs on the SH break at lower altitudes and the GW drag in the upper mesosphere is reduced (Yasui et al., 2016).
According to the theory, GW activity in the upper mesosphere should reduce in the time after an SSW event (with 4-10 days shift) and it should increase below. A negative anomaly of the mean meridional wind should also be observed (Yasui et al., 2016).

Chapter 2

Methodology

2.1 Superposed epoch analysis

The average meteorological conditions during SSW events should be characterized in this project. Thus, this project does not aim to investigate the differences between individual events. It rather concentrates on the mean perturbations to be expected during an "average" SSW event.
Therefore a method which is called "superposed epoch analysis" (sometimes known as composite analysis as well) was used. At that the data from each event are ordered with reference to the so-called "epoch time" (Denton et al., 2019). In this case this is the time of the SSW onset. These ordered data were then averaged over all considered SSW events in order to receive the average conditions. These were then plotted for a time period from 30 days before to 30 days after the SSW onset. The dates at which SSW events occured were extracted from Denton et al. (2019) and King et al. (2019).
To investigate anomalies as well, the deviation relative to the climatologies for the same calendar day was derived.

Chapter 3

Data

The data used in this project consist of meteor radar measurements and model simulations of the whole atmosphere model GAIA for five stations. The location of these stations is shown in Fig. 3.1. Three of them - Kiruna, Collm Observatory and the CMOR meteor radar at London, Ontario (further referred to as CMA) - are situated on the NH. Whereas Rio Grande and Davis are located on the SH. Because of the different lengths of the time series at the five stations not all SSW events could be investigated at each station. The data availability of the different stations and the corresponding number of SSWs included in the analysis is shown in table 3.1.

3.1 Meteor radars

Meteor radars do not measure radar signals of a meteor itself but those reflected by the gas trail it leaves behind on his way through the earth's atmosphere.
Due to the extremely high velocities at which meteoroids enter the atmosphere (up to $72,000\,\mathrm{km\,h^{-1}}$), a large amount of kinetic energy is transformed into frictional heat as the meteor is moving through the denser atmosphere. By heating to extremely high temperatures, the gas left behind is highly ionised. In contrast to the neutral background atmosphere this ionised gas trail reflects the radar signals emitted by the meteor radar. Then the Doppler-shift of the detected signal is analysed in order to derive the horizontal wind speed (Wilhelm et al., 2017).
As the intensity of the reflected signals depends on the number of measurable meteors, only the altitude range where these ionisation processes take place can be measured with a meteor radar (Wilhelm et al., 2017). In the case of the radar data analysed in this project this altitute range extends from around 70 to 100 km. The data points at the edges above and below these boundaries are not fully reliable and must therefore be treated with caution.

3.2 Ground-to-topside model of Atmosphere and Ionosphere for Aeronomy (GAIA)

The Ground-to-topside model of Atmosphere and Ionosphere for Aeronomy (GAIA) is a whole atmosphere model, which allows to study the effects of the lower atmosphere on upper atmosphere layers up to the ionosphere. Therefore GAIA uses three sub-models (Jin et al., 2011).
An atmospheric general circulation model (0 - 600 km) includes tropospheric processes, photochemical reactions in the thermosphere and interactions between the neutral atmosphere and

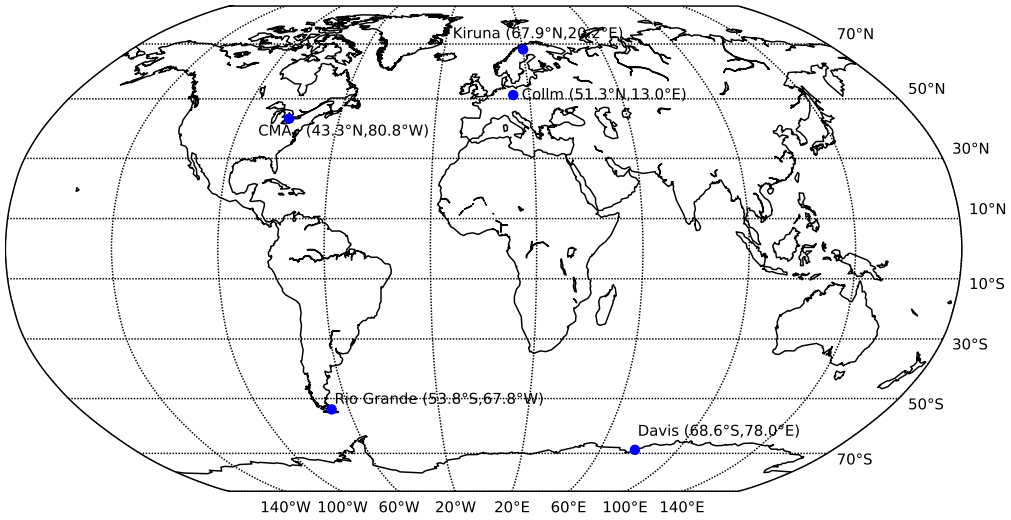

Figure 3.1: Locations of the meteor radar stations - marked with a blue dot. The coordinates of latitude and longitude are printed next to the station name.

Table 3.1: Start and end dates of the time series of the meteor radar data and the number of SSW events included in the analysis for the different stations.

Station	Start	End	Number of SSWs
Kiruna	01.08.1999	31.12.2019	27
Collm	01.08.2004	06.03.2019	19
CMA	01.01.2002	31.12.2018	22
Rio Grande	01.02.2008	31.12.2019	13
Davis	01.01.2005	31.12.2019	19

the ionosphere (Jin et al., 2011).
An ionospheric plasma fluid model simulates the dynamics in the altitude range from 100 to 3000 km and features photochemical reactions of the available ions (Jin et al., 2011).
As a third part an electrodynamics model simulates ionospheric currents and electric fields produced by charged particle flows in the thermosphere. All together the three sub-models form a complex model for the whole atmosphere - GAIA (Jin et al., 2011).

Chapter 4

Results

4.1 Wind

4.1.1 Collm and Kiruna

Kiruna (67.9° N, 20.2° E) and Collm (51.3° N, 13° E) are the two northernmost stations and therefore treated first. Fig. 4.1 represents composites of the measurements of the zonal wind component at Collm and Kiruna. The upper panels - i.e. Fig. 4.1(a) and Fig. 4.1(b) - represent the absolute composite average. The lower panels - i.e. Fig. 4.1(c) and Fig. 4.1(d) - represent its anomalies.
In the time period from 3 weeks until 1 week before the SSW the zonal wind is more westerly (eastward) than normal (in the mean for the certain calendar day). This could be the upper edge of the intensified jetstream between stratosphere and mesosphere, which is typical in the time before SSWs. That was validated with GAIA model data in section 4.3.
Around 4 to 5 days before the onset of the SSWs the zonal wind becomes less westerly and maybe even gets a weak easterly (westward) component. This wind drop is typical for the SSW onset as the polar vortex and the stratospheric jet collapse.
At Kiruna an very strong increase in the u-component as well as in the anomalies is pronounced around 20-30 days after the SSW onset between 75 and 85 km. This observation could correspond to the re-establishment of the stratopause, which often takes place in this height some weeks after an SSW event. This was also validated with GAIA model data (see section 4.3).
In the altitude range from 90 to 100 km the zonal wind becomes more easterly with the beginning of the SSW and already around one week before the onset (more pronounced at Collm).

The measurements of the meridional wind component at Collm and Kiruna are shown in figure 4.2(a) and Fig. 4.2(b). The anomalies are shown in Fig. 4.2(c) and 4.2(d).
On the day of the SSW onset we see a change in the meridional wind direction from southern (northward) to northern (southward). After the SSW onset positive meridional-wind anomalies return.
In Kiruna the negative anomalies and the increasing northern (southward) direction of the meridional wind component are spread wider concerning time compared to the Collm observatory. They begin around 2-3 days before the onset of the SSWs and last until 2-3 days after it as well.
The cause of this behaviour of the meridional wind is explained below.

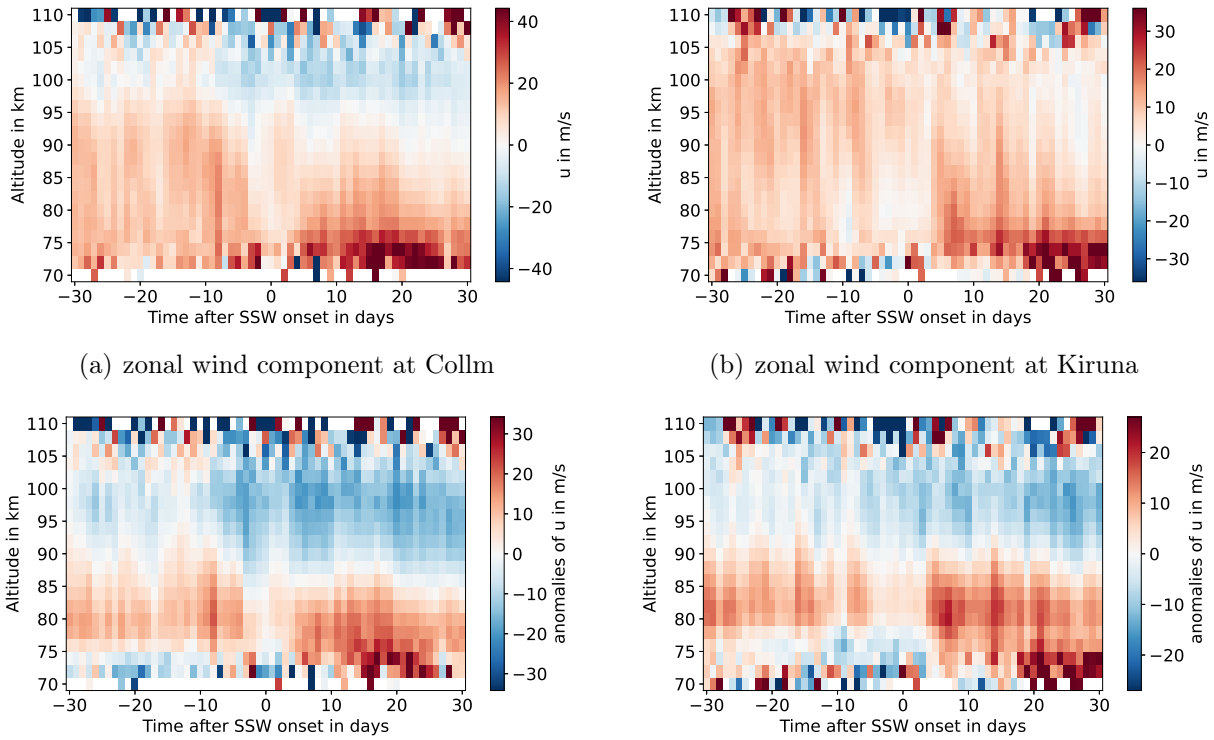

(a) zonal wind component at Collm

(b) zonal wind component at Kiruna

(c) anomalies of the zonal wind component at Collm

(d) anomalies of the zonal wind component at Kiruna

Figure 4.1: Measurements and anomalies of the zonal wind component by meteor radars at Collm observatory (left) and Kiruna (right).

As shown before, the eastward zonal wind decreases during an SSW event.
On the one hand this leads to a Doppler-shifting of the westward propagating GWs (negative phase speeds) towards shorter vertical wavelengths. As a result they break at lower altitudes. On the other hand GWs with high positive phase speeds can propagate further upward into the mesosphere as they are not filtered anymore. Because of these processes the westward GW drag is both reduced and downward shifted in the winter mesosphere (Körnich and Becker, 2010). Thus the poleward meridional flow on the NH weakens. This means that the meridional winds become less southern (northward) and may even reverse to southward directions. It results in the observed negative anomaly of the mean meridional wind speed.

4.1.2 CMA

The meteor radar station in London, Ontario (Canada) shows the decrease of the westerly (eastward) component in 70 to 80 km not as well pronounced as at Collm and Kiruna (cf. Fig. 4.3(a)). But in higher altitudes between 90 and 110 km we see around 4-5 days before the SSW onset the zonal wind becoming more easterly (westward). Especially the anomalies in Fig. 4.3(c) show that, whose signature descends in altitude with propagating time. As there was no signature in GWs this decrease could probably be caused by planetary waves.
At CMA the v-component of the wind shows a strong increase and positive anomaly in the mesosphere around a week before the SSW onset (cf. Fig. 4.3(b)). Besides, around 10 - 7

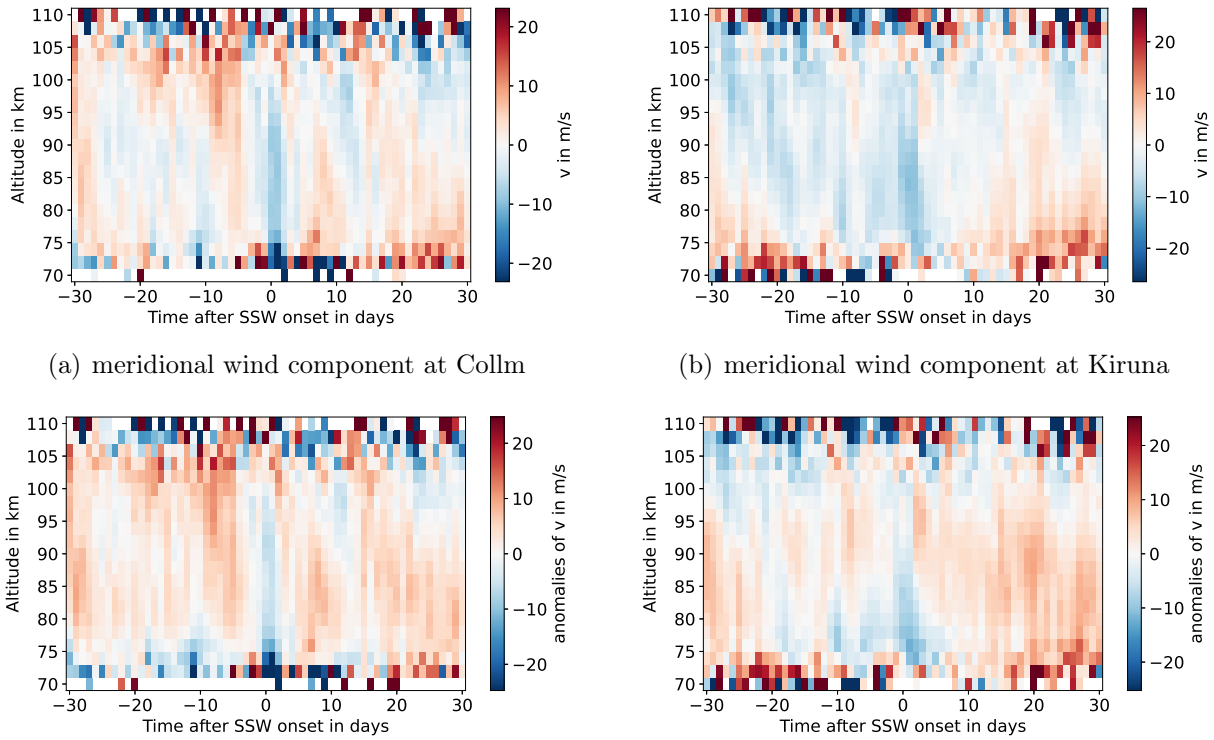

(a) meridional wind component at Collm

(b) meridional wind component at Kiruna

(c) anomalies of the meridional wind component at Collm

(d) anomalies of the meridional wind component at Kiruna

Figure 4.2: Measurements and anomalies of the meridional wind component by meteor radars at Collm observatory (left) and Kiruna (right).

days before the SSW onset and during the 10 days after the SSW onset the northward wind is much weaker and at some point already turns to a weak southward component. This is opposing to the results obtained for the other two stations on the NH. The reason of the wind vacillation may be attributed to PWs as there is no signature in the GW activity. This needs to be investigated in another project.

4.1.3 Rio Grande

We also consider two stations in the SH, i.e. Rio Grande and Davis.

At the radar station at Rio Grande in Argentina the zonal wind speeds tend to decrease in magnitude (in both directions) after the onset of the SSWs (see Fig. 4.4(a)). The easterlies in around 80 km become less easterly and the westerlies between 90 and 100 km become less westerly. The mesospheric change in around 80 km altitude is exactly the zonal wind decrease which was expected by the theory of inter-hemispheric coupling. But all in all the winds are still stronger than in the climatological mean for the corresponding calendar day as the anomalies of the zonal wind show in Fig. 4.4(c).

The meridional wind component shows multi-day fluctuations appearing as stripes in Fig. 4.4(b), which decrease in magnitude with the SSW onset. And around 10 days after the SSW

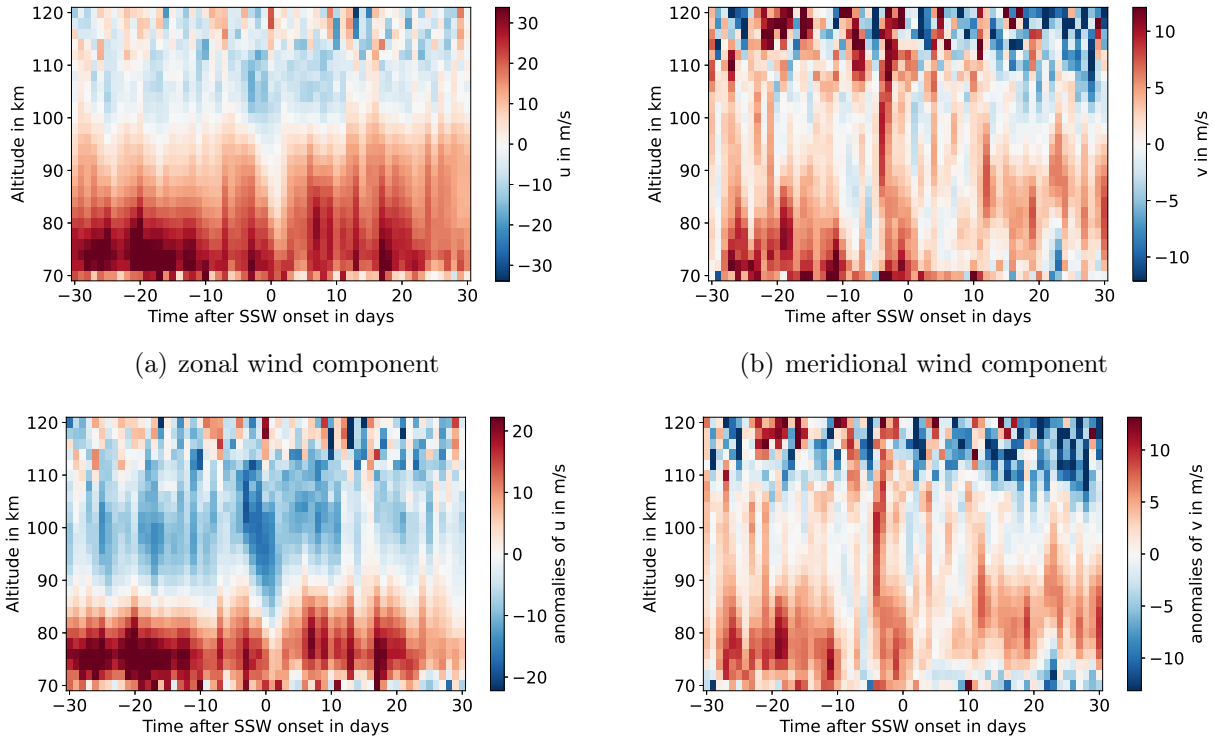

(a) zonal wind component

(b) meridional wind component

(c) anomalies of the zonal wind component

(d) anomalies of the meridional wind component

Figure 4.3: Measurements and anomalies of the zonal and meridional wind component by the meteor radar at CMA station.

onset the meridional wind reverses to a southward direction. This reversal is associated with the negative anomalies in the meridional wind component (see Fig. 4.4(d)) which were expected by the inter-hemispheric coupling theory as well.

4.1.4 Davis

At Davis these inter-hemispheric coupling impacts are less pronounced. The results for Davis station are shown in Fig. 4.5. There are only very slight changes in the zonal wind component and the anomalies are of small magnitude.
In general, Davis shows the least changes of the 5 stations. This seems logic as it is situated in the Antarctic and therefore is the southernmost station with the greatest distance to the northern hemispheric polar vortex where the SSW events occur.

4.2 Gravity waves

Concerning the GWs we see a different behaviour for both hemispheres. The meteor radars on the NH (Collm, Kiruna, CMA) show an increased level of GW kinetic energy before and around - maybe short time after, too - the onset of the SSWs. Later the activity of GWs reduces to the normal climatological amount.
On the SH (Rio Grande, Davis) the GWs are at a low level before the SSW-onset. Approx-

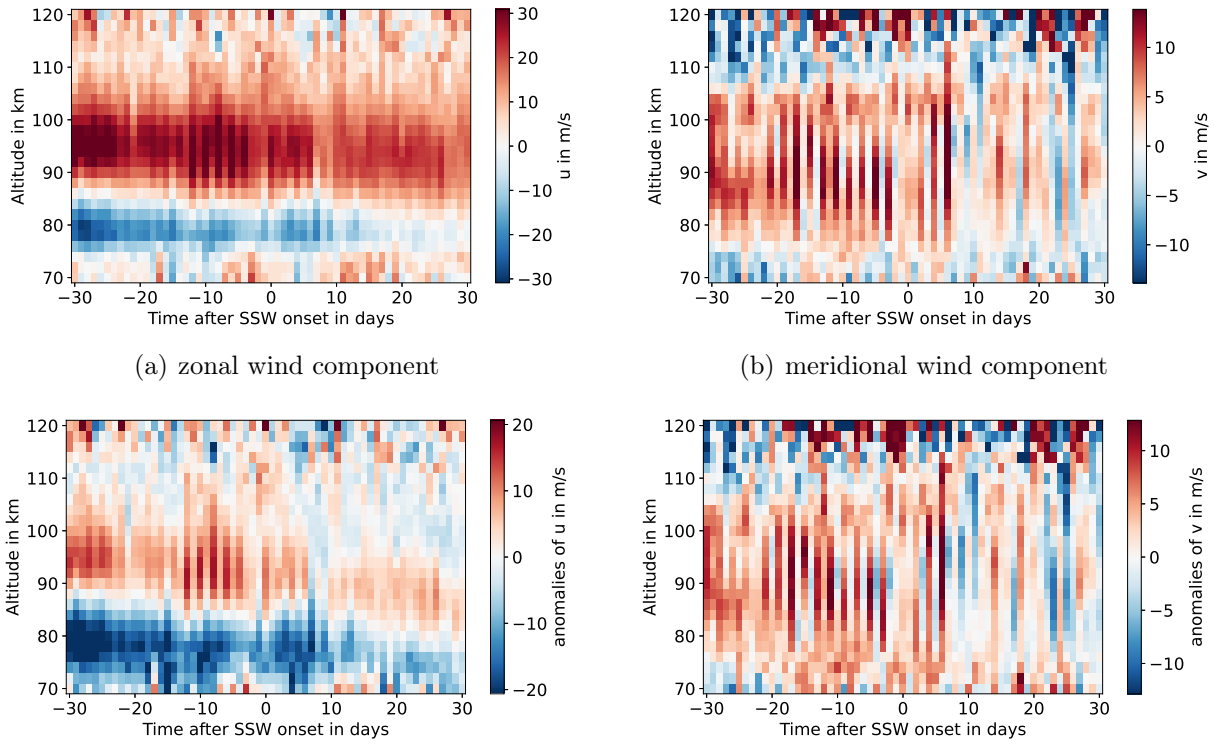

(a) zonal wind component

(b) meridional wind component

(c) anomalies of the zonal wind component

(d) anomalies of the meridional wind component

Figure 4.4: Measurements and anomalies of the zonal and meridional wind component by the meteor radar at Rio Grande station.

imately 2 to 3 weeks afterwards the kinetic energy is significantly increased compared to the climatological mean. These results are discussed in detail in the next subsections.

4.2.1 Northern hemisphere (Collm, Kiruna, CMA)

At first the situation on the NH is presented. After the onset of the SSW the kinetic energy of the GWs shows a slight decrease at Collm Observatory in Fig. 4.6(a). This would mean that around and after SSWs less or at least weaker GWs are present in the mesosphere. Especially the zonal component of the GWs shows this decrease as well.
But when we look in the plot of the anomalies (see Fig. 4.6(c)), it can be seen that the lower GW activity after the SSW onset is normal with respect to the climatology, while the higher activity during the 60 days before the SSWs is anomalous (high anomalies). This means that the radar observations show an increased level of GW activity in altitudes between 85 and 95 km during the 2 months before the onsets of the SSWs.

Kiruna paints a similar picture while the CMOR Meteor radar (CMA) measures the increases in GW activity before the SSWs with weaker magnitude (the increase and the anomalies are less pronounced). This can be seen in Fig. 4.6(b) and (d).

So it can be concluded that on the NH there is an enhanced level of GW kinetic energy before the SSW onset.

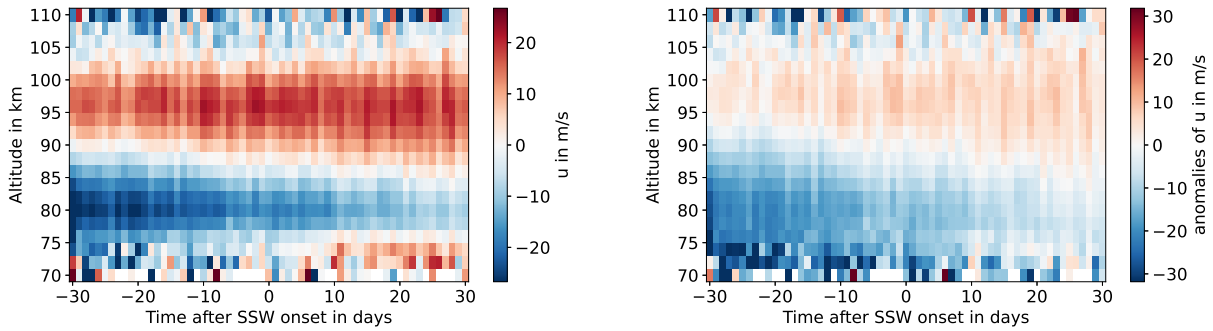

(a) zonal wind component

(b) anomalies of the zonal wind component

Figure 4.5: Measurements and anomalies of the zonal wind component by the meteor radar at Davis station.

The reason therefore could be the jetstream, which intensifies typically before the beginning of an SSW event. Because of the increased wind speed the GW filtering is changed in that way, that more waves with larger positive phase speeds are filtered and can't propagate further upward to the mesosphere. As a result there are less GWs with positive phase speed in the mesosphere. Because of that, the GWs with negative phase speed predominate even more than normal. Thus the zonal GW component (which is defined as the difference between the positive and negative zonal GW components) becomes absolute more negative (according to amount greater). Hence the total kinetic energy of GWs increases. This leads to the observed enhanced GW activity in higher altitudes (here: 85 - 95 km).

4.2.2 Southern hemisphere (Rio Grande, Davis)

On the SH the situation is vice-versa. The climatologies and anomalies of Rio Grande and Davis are shown in Fig. 4.7. Before the SSW onset GWs are at low level at Rio Grande and Davis. Approximately 2 to 3 weeks afterwards the kinetic energy is significantly increased compared to the climatological mean.
These findings according to anomalies of GW kinetic energy at Davis and Rio Grande seem to be consistent with the theoretical expectation from the inter-hemispheric coupling theory. One can see negative anomalies in around 90 km altitude before or around SSW events and positive anomalies below. And the decreasing kinetic energy of GWs in the upper mesosphere around the SSW onset is visible in the climatology plot as well. Especially at Davis this is well pronounced (see Fig. 4.7(b)).
This agreement with the theory is an advance compared the a study of Yasui et al. (2016) as their obtained results were inconsistent with the inter-hemispheric coupling hypothesis.

4.3 GAIA data

As a kind of validation the results of the runs of the whole atmosphere model (GAIA) for the considered stations were investigated, too. How the model agrees with the measurements is presented in this section. Thereby the investigations were restricted to the two northernmost

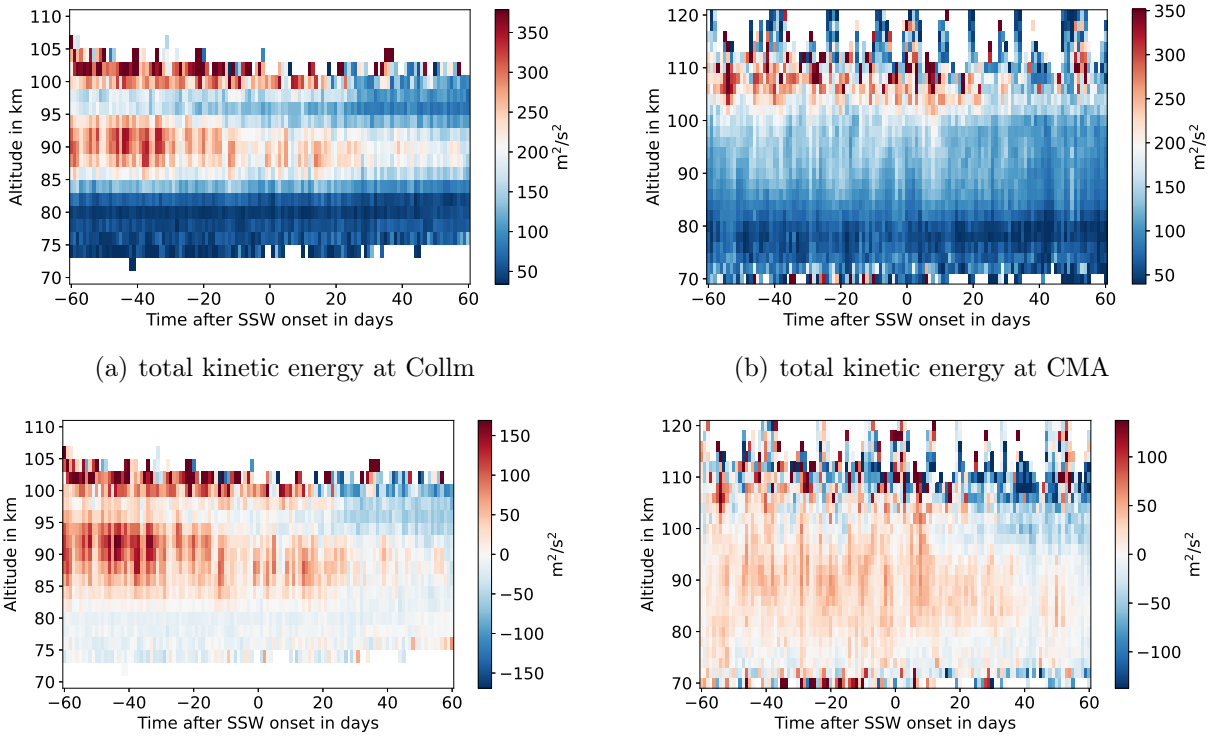

(a) total kinetic energy at Collm

(b) total kinetic energy at CMA

(c) anomalies of the total kinetic energy at Collm

(d) anomalies of the total kinetic energy at CMA

Figure 4.6: Total kinetic energy of the gravity waves at Collm Observatory and CMA station.

stations - Collm and Kiruna.

4.3.1 Zonal wind

The GAIA model simulations for the u-component of the wind are presented in Fig. 4.8 and show an anomalously high intensity of the polar stratospheric jet stream (around 50 km altitude) in the month before the SSW onsets. The anomalies of the zonal wind speed show values of up to 50 $\mathrm{m\,s^{-1}}$ in comparison to the climatological mean values for the corresponding calendar day. This zone of enhanced wind speed around the intensified stratospheric jet ranges with its edges from 30 km up to 80 km. Hence this seems to be the reason for the enhanced zonal wind speed in the mesosphere, which was observed by the Collm meteor radar in the month before the onsets of the SSWs (see section 4.1.1).
Ongoing from 10 days before the SSW onset the zonal wind gets less westerly especially in an altitude range from 40 to 60 km (around the altitude of the stratospheric jet in 50 km). At Kiruna it even reverses and shows a slight easterly component in the days around the SSW onset.
But even in the atmospheric layers between 60 and 80 km the zonal wind gets less westerly. The reason therefore is the enhanced easterly GW activity in the mesosphere, which is generated by the increased critical-layer filtering because of the intensified stratospheric jet stream in the month before the SSW onset (was shown above). This westward GWs propagate up to the mesosphere and reach high amplitudes because of the exponentially decreasing density and break because of that. When they break, they generate easterly winds, which (over-)compensate

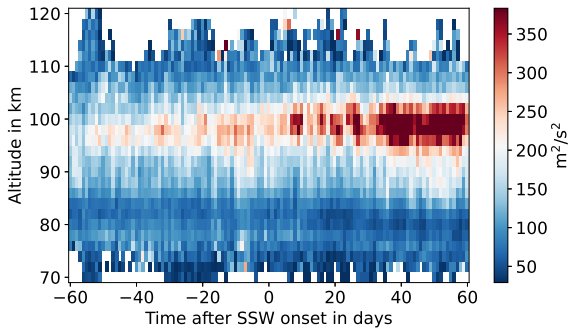

(a) total kinetic energy at Rio Grande

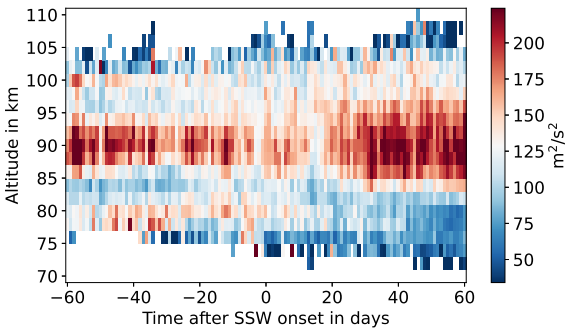

(b) total kinetic energy at Davis

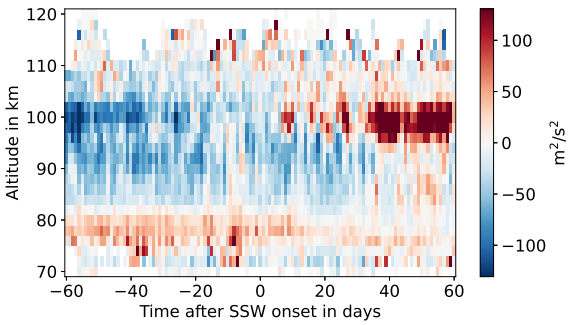

(c) anomalies of the total kinetic energy at Rio Grande

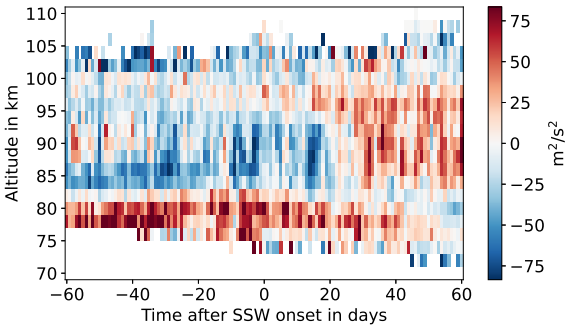

(d) anomalies of the total kinetic energy at Davis

Figure 4.7: Total kinetic energy of the gravity waves at Rio Grande and Davis station.

the normal westerly flow.
In the month after the SSW onset this zone of anomalously low westerly zonal winds descends in the middle and lower stratosphere (20 - 40 km). Above, the westerly zonal winds are stronger than normal. This phenomenon refers to the so-called "elevated stratopause", which sometimes re-establishes in altitudes of 60 - 80 km after an SSW event and descends gradually to normal altitudes afterwards. Here GAIA agrees with the Collm and Kiruna meteor radars, which observed anomalously strong westerly winds in altitudes from 70 - 80 km as well.
As this feature can be seen in the SSW climatologies as well of the radar observations as of the GAIA simulations, it seems likely that an elevated stratopause (ES) event occurs often after an SSW event.

4.3.2 Meridional wind

The meridional wind reversal from southern (northward) to northern (southward) around the onset of the SSW events, which was observed by the Collm and Kiruna meteor radars, is reproduced by the GAIA model as well (see Fig. 4.9).
Another interesting feature is the strong increase of the northward winds in 40 - 70 km altitude in the month before the SSW onset. This phenomenon was even more pronounced in the model runs for the Kiruna station than it was in the ones for the Collm station.

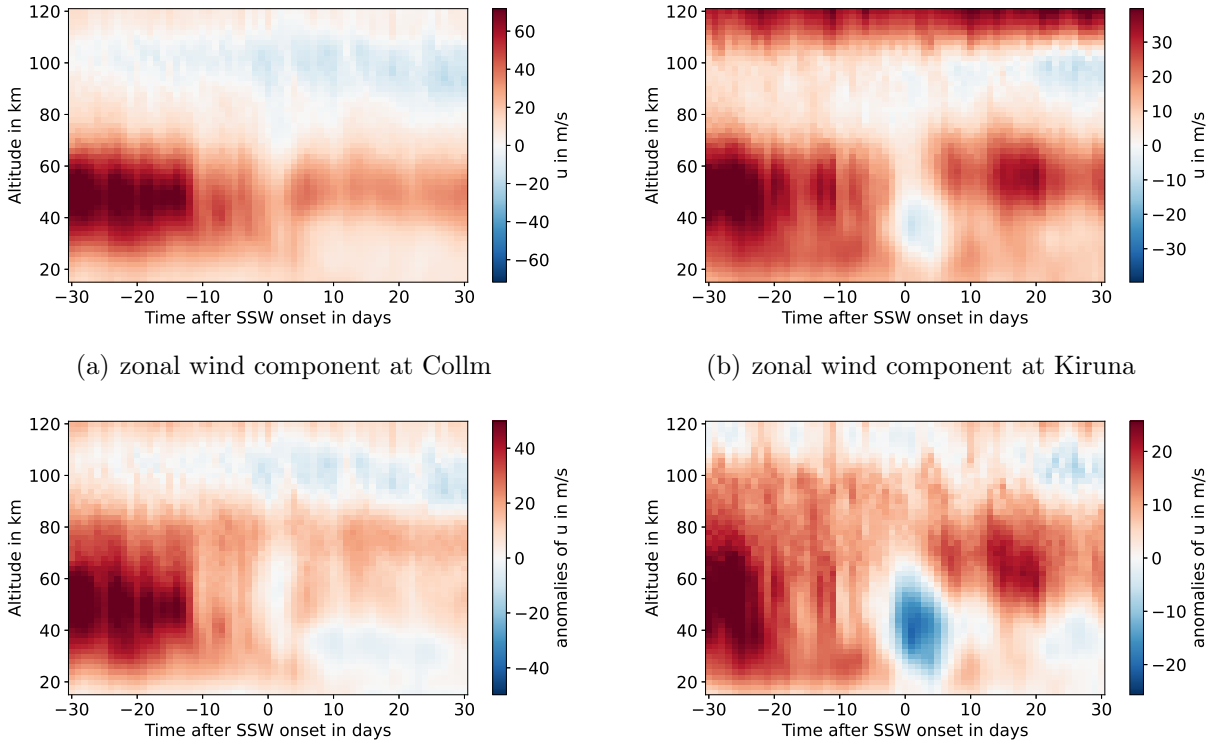

(a) zonal wind component at Collm

(b) zonal wind component at Kiruna

(c) anomalies of the zonal wind component at Collm

(d) anomalies of the zonal wind component at Kiruna

Figure 4.8: GAIA model data of the zonal wind component at Collm Observatory and Kiruna station.

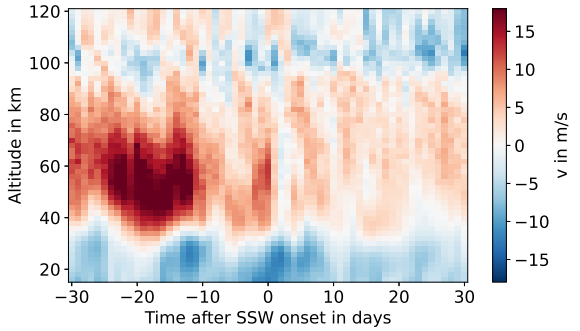

(a) meridional wind component at Collm

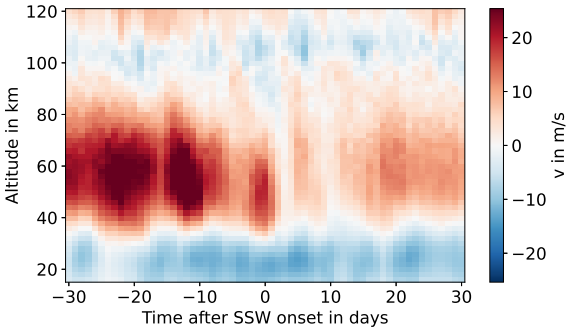

(b) meridional wind component at Kiruna

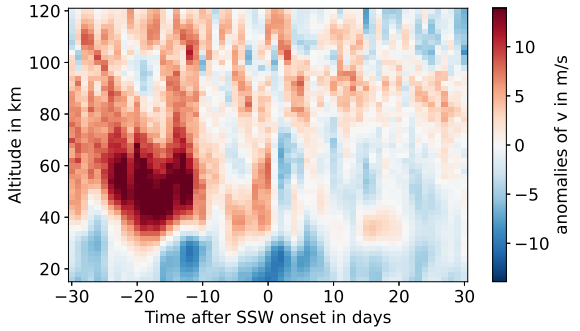

(c) anomalies of the meridional wind component at Collm

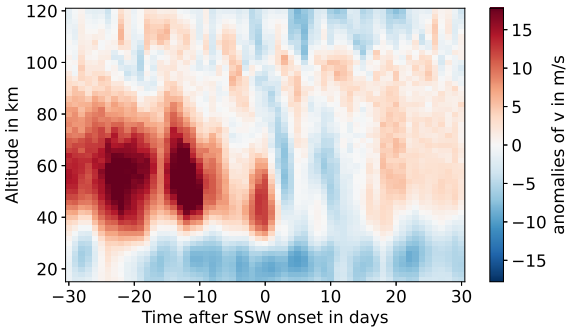

(d) anomalies of the meridional wind component at Kiruna

Figure 4.9: GAIA model data of the meridional wind component at Collm Observatory and Kiruna station.

Chapter 5

Conclusion

This student project aimed to analyse the mean meteorological conditions in the time period around SSW events at different locations on the NH as well as on the SH. This was achieved by analysing meteor radar measurements of wind speed at 5 stations using the superposed epoch analysis method.

The results showed a strong latitudinal dependence of the SSW effects. On the NH an enhanced GW activity was observed in the upper mesosphere before an SSW event. These GWs are - besides the planetary waves - an important driver for the mesospheric circulation. Furthermore, both the meteor radar data and GAIA data suggest that an elevated stratopause seems to be a common phenomenon after SSW events.

With lower geographical latitude (i.e., growing distance to the NH polar vortex) the SSW effects appeared to be weaker. The results which were found for the stations on the SH are consistent with the inter-hemispheric coupling theory.

To unterstand all effects, planetary waves need to be investigated, too. They initiate the SSW events and have an considerable impact on the mesospheric circulation as well.

Bibliography

Chandran, A., Collins, R., and Harvey, V. (2014). Stratosphere-mesosphere coupling during stratospheric sudden warming events. *Advances in Space Research*, 53(9):1265 – 1289.

Denton, M., Kivi, R., Ulich, T., Rodger, C., Clilverd, M., Denton, J., and Lester, M. (2019). Observed response of stratospheric and mesospheric composition to sudden stratospheric warmings. *Journal of Atmospheric and Solar-Terrestrial Physics*, 191:105054.

Jin, H., Miyoshi, Y., Fujiwara, H., Shinagawa, H., Terada, K., Terada, N., Ishii, M., Otsuka, Y., and Saito, A. (2011). Vertical connection from the tropospheric activities to the ionospheric longitudinal structure simulated by a new Earth's whole atmosphere-ionosphere coupled model. *Journal of Geophysical Research: Space Physics*, 116(A1).

King, A. D., Butler, A. H., Jucker, M., Earl, N. O., and Rudeva, I. (2019). Observed relationships between sudden stratospheric warmings and european climate extremes. *Journal of Geophysical Research: Atmospheres*, 124(24):13943–13961.

Körnich, H. and Becker, E. (2010). A simple model for the interhemispheric coupling of the middle atmosphere circulation. *Advances in Space Research*, 45(5):661 – 668.

McLandress, C. (1998). On the importance of gravity waves in the middle atmosphere and their parameterization in general circulation models. *Journal of Atmospheric and Solar-Terrestrial Physics*, 60(14):1357 – 1383.

Wilhelm, S., Stober, G., and Chau, J. L. (2017). A comparison of 11-year mesospheric and lower thermospheric winds determined by meteor and MF radar at 69 N. *Annales Geophysicae*, 35(4):893–906.

Yasui, R., Sato, K., and Tsutsumi, M. (2016). Seasonal and interannual variation of mesospheric gravity waves based on MF radar observations over 15 years at Syowa station in the Antarctic. *SOLA*, 12:46–50.

List of Figures